

Product Costing in Data Pipelines

Li Peng^{1,2}, Jie You², Feng Shi³, Yihang Wu¹, Jianxin Wang³, Weiran Liu²,

Xinyu Peng^{1,2}, Junhua Wang², Lei Zhang², Lin Qu², Jinfei Liu¹

¹Zhejiang University ²Alibaba Group ³Central South University

¹{jerry.pl, steven.pengxy}@alibaba-inc.com, {yhwu_is, jinfeiliu}@zju.edu.cn

²{youjie.yj, weiran.lwr, junhua.wjh, zongchao.zl, xide.ql}@alibaba-inc.com

³{fengshi, jxwang}@csu.edu.cn

ABSTRACT

In data-intensive enterprises, data pipelines are essential for transforming raw data into valuable data products. To provide a sound basis for data pricing and cost optimization, enterprises usually perform *product costing*, which apportions the total cost of all resources (e.g., CPU, Memory) consumed within pipelines to data products. However, product costing in data pipelines faces significant challenges not encountered in traditional physical pipelines, including the non-rivalrous nature of data that complicates the costing formulation, the prevalence of cyclic dependencies that distort the accuracy of results, and the massive scale of pipelines that leads to computational intractability.

In this paper, for the first time, we formalize the problem of product costing in data pipelines as a *manufacturing cost of data products (MCP) problem* to overcome the non-rivalrous nature of data. To solve MCP, we propose CostApp, a hybrid algorithm that achieves both exactness and scalability, even for cyclic and massive-scale pipelines. CostApp performs a dimensionality reduction by isolating cyclic dependencies via a feedback arc set (FAS). It aggregates costs onto a compact set of key vertices using a scalable iterative approach, transforming the intractable computational problem into a reduced linear system that can be solved exactly and efficiently by a basic matrix-based method. Experiments on both real-world data from Alibaba and synthetic data show that CostApp scales to process a production pipeline with over 28 million entities within one hour while preserving exactness, supporting pipelines up to $10^3 \times$ larger than the direct matrix-based baseline. We open-source both the Alibaba pipeline dataset and the implementation to facilitate future research.

PVLDB Reference Format:

Li Peng^{1,2}, Jie You², Feng Shi³, Yihang Wu¹, Jianxin Wang³, Weiran Liu², Xinyu Peng^{1,2}, Junhua Wang², Lei Zhang², Lin Qu², Jinfei Liu¹. Product Costing in Data Pipelines. PVLDB, 14(1): XXX-XXX, 2020.

doi:XX.XX/XXX.XX

PVLDB Artifact Availability:

The source code, data, and/or other artifacts have been made available at URL_TO_YOUR_ARTIFACTS.

This work is licensed under the Creative Commons BY-NC-ND 4.0 International License. Visit <https://creativecommons.org/licenses/by-nc-nd/4.0/> to view a copy of this license. For any use beyond those covered by this license, obtain permission by emailing info@vldb.org. Copyright is held by the owner/author(s). Publication rights licensed to the VLDB Endowment.

Proceedings of the VLDB Endowment, Vol. 14, No. 1 ISSN 2150-8097.
doi:XX.XX/XXX.XX

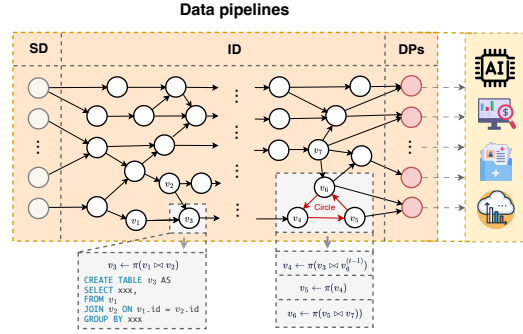


Figure 1: An illustration of data pipelines, where π denotes a join operation. $v_i^{(t-1)}$ represents the version of data entity v_i from the previous day, while entities without superscripts denote the current day's version.

1 INTRODUCTION

Over the past decades, the pervasive adoption of data-driven decision-making has established data as a critical asset [2, 24]. With both data volume and demand rising sharply, deriving value from data increasingly depends on the ability to process and refine it at scale. To transform large amounts of raw data into valuable data products, large data-intensive enterprises (e.g., Google, Meta, and Alibaba) have built extensive data pipelines [3, 4, 21, 42]. These pipelines ingest diverse data sources and coordinate complex production dependencies to create a wide array of valuable data products that support business-critical scenarios, from operational decision-making to machine learning applications [29, 42, 44, 48, 49].

Data pipelines in data-intensive enterprises are characterized by *consolidation* and *periodicity*, presenting requirements for costing. Data is *non-rivalrous in consumption* [23, 37, 47]—it can be consumed repeatedly without depletion. To leverage this, enterprises integrate processing from numerous business domains into a *consolidated* digital supply chain, allowing frequently accessed data to be shared across multiple downstream products to maximize reuse value. Consolidated pipelines weave thousands of lineages together, creating a complex, many-to-many dependency graph. As shown in Fig. 1, source data (SD) is progressively refined through transformations into intermediate data (ID) and, finally, into valuable data products (DPs) ready for use across various businesses. These consolidated pipelines consume massive resources (e.g., CPU, Memory), presenting requirements for cost accounting. Furthermore, these pipelines operate with workload *periodicity*, typically executing recurrently (e.g., daily extract-transform-load (ETL) jobs) to keep data up-to-date. This continuous and cumulative resource consumption means that even modest unit costs aggregate into substantial financial

expenditures over time. For example, at Alibaba, data pipelines processing terabytes of daily data incur resource costs equivalent to millions of dollars annually. Consequently, the interplay of complex consolidated dependencies and long-term periodic consumption makes cost visibility a necessity for operating data pipelines.

While resource consumption is distributed across all data entities (SD, ID, DP), business value is delivered exclusively through the final DPs (via monetization or usage). Thus, DPs constitute the natural unit for financial accountability. We term this *product costing in data pipelines*—apportioning the total costs of all resources consumed within pipelines to final DPs. This costing provides the necessary basis for data pricing [15, 37] and pipeline optimization [29, 48], yet it remains largely unexplored in existing literature.

Table 1: Comparison of physical and data pipelines.

	Physical pipelines	Data pipelines	Unique challenges
Consumption feature of outputs	rivalrous	non-rivalrous	consumption-based costing not applicable, complicates cost modeling
Type of dependencies	acyclic	cyclic	result accuracy of propagation-based solutions is distorted
Scale	small	large	costing solutions with exactness guarantee may be computationally intractable.

Challenges. However, product costing in data pipelines presents unique challenges not encountered in physical pipelines, as summarized in Tab. 1.

First, data’s inherent *non-rivalrous nature in consumption* [23, 37, 47] fundamentally challenges cost modeling. In physical manufacturing pipelines, intermediate outputs are typically rivalrous physical goods. The costs embedded in a unit of a physical good are fixed (typically as its marginal cost) and fully transferred downstream upon its consumption. For example, when a car part is used in assembling a vehicle, its cost is fully attributed to that vehicle. Thus, consumption-based costing in physical pipeline naturally upholds the principle of *completeness* [1], meaning *all* consumed resources are fully accounted for within the costing *without duplication*. However, in data pipelines, data is not depleted when used, resulting in (nearly) zero marginal cost for each additional consumption [37]. Applying traditional costing creates a dilemma: allocating based on marginal cost [40] leads to severe under-costing, while charging the full cost to every consumer results in massive over-costing, both of which violate completeness. This difficulty challenges the formulation of a cost model that guarantees completeness of costing.

Second, the workload periodicity of data pipelines leads to a time-versioned nature of data entities, inevitably introducing *cyclic dependencies* in the lineage graph. For instance, a daily user profile update often requires joining new behavioral data with its own previous snapshot, structurally forming a self-dependency or cycle in the lineage graph. Beyond self-loops, complex multi-hop cycles also arise, such as the loop formed by vertices v_4, v_5 , and v_6 in Fig. 1, where v_4 relies on $v_6^{(t-1)}$, the version of v_6 from the previous day ($v_4 \leftarrow \pi(v_3 \bowtie v_6^{(t-1)})$). Such cycles are pervasive in production

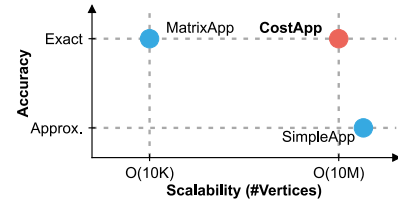


Figure 2: Approaches for product costing in data pipelines.

pipelines. They cause basic cost allocation methods based on topological propagation (see §3.3.1) to fail, as costs circulate indefinitely within loops rather than being fully attributed to final data products. Without proper handling, this leads to significant calculation errors that may mislead pricing strategies or undermine cost optimization efforts.

Third, the consolidation of data pipelines results in a *massive scale* of data entities. While traditional physical supply pipelines typically manage a limited number of entities (e.g., thousands of intermediate units), a consolidated data pipeline at large enterprises often comprises tens of millions of data entities with complex dependencies e.g., 28 million vertices at Alibaba. At this scale, solutions for exact costing may become computationally intractable. Specifically, direct algebraic solutions (see §3.3.2) typically require matrix inversion with $O(|V|^3)$ time complexity. For graphs with millions of vertices, such cubic complexity is prohibitive. Therefore, a practical cost calculation method must be inherently scalable and designed to operate efficiently in a distributed environment.

Contributions. To address these challenges, this paper makes the following contributions:

First, to resolve the dilemma caused by non-rivalrous consumption of data, we formalize the problem of product costing as the manufacturing cost of data products (MCP) problem. Unlike the consumption-based approach, we adopt a ratio-based cost model governed by the cost conservation property (Definition 1 in §3). This formulation guarantees completeness of product costing, ensuring precise cost apportionment to final data products without the under-costing or duplication pitfalls of traditional approaches. To resolve MCP problem, we propose two basic solutions: SimpleApp, a distributed, propagation-based algorithm that scales to large pipelines but only yields approximate results, and MatrixApp, which provides an exact solution via matrix inversion but is limited to small pipelines. These basic solutions highlight the fundamental trade-off between exactness and scalability, serving as building blocks for our hybrid approach.

Second, we propose CostApp, a hybrid algorithm that achieves both exactness and scalability by strategically integrating our basic methods. The core idea is to decouple the computational complexity by isolating cyclic dependencies. Specifically, CostApp first identifies a feedback arc set (FAS) and strategically inserts auxiliary sink and source vertices on these arcs to isolate these cycles. It then employs the scalable SimpleApp on the resulting acyclic graph to efficiently aggregate costs onto these auxiliary sink vertices and the final data products. This aggregation transforms the problem into a reduced linear system while preserving the final manufacturing cost of data products, which is then solved exactly using MatrixApp. This effectively performs a *dimensionality reduction*,

shifting the bottleneck from inverting a massive $|V| \times |V|$ matrix (where $|V|$ is millions) to inverting a tiny matrix sized proportional to the feedback arcs (often $< 0.1\%$ of $|V|$). This approach allows us to achieve exact results with high scalability simultaneously. A comparison that highlights its strengths is outlined in Fig. 2.

Third, we implement CostApp and conduct comprehensive experiments on both real-world data from Alibaba and synthetic data. Results demonstrate that CostApp successfully reduces a computationally prohibitive problem to a solvable one, achieving both result exactness and high scalability that outperform baselines. It successfully processes a production pipeline graph with over 28 million entities in an hour and has been successfully deployed in Alibaba’s production environments.

To the best of our knowledge, we are the first to formalize the problem of product costing in data pipelines and to propose a scalable, exact solution. Our contributions are summarized as follows:

- We formalize the data manufacturing cost problem in data pipelines and propose two basic solutions for this problem: one exact for small pipelines and one approximate for large ones.
- We propose CostApp, a novel hybrid algorithm that provides exact and scalable manufacturing cost calculation.
- We validate CostApp’s superiority through extensive experiments on both real-world and synthetic data. We open-source our real data pipeline dataset and implementation to facilitate future research.

2 PRELIMINARY

In this section, we introduce the background knowledge of data pipelines and Pregel-based distributed computation.

2.1 Data Pipelines

In this paper, we focus on *consolidated* data pipelines that consolidate numerous data transformation tasks (*e.g.*, SQL queries, MapReduce jobs) across diverse business domains for centralized management. Such pipelines are widely adopted by large data-intensive enterprises [3, 4, 42]. Their primary objective is to generate DPs through a sequence of data transformation operations. Typically, these jobs execute in batch mode: reading source data from storage, performing transformations (*e.g.*, cleaning, joining, aggregation, and feature extraction), and persisting the results back to storage. Formally, we denote a processing operation as o , which consumes a set of input data entities to produce a single output data entity. For instance, regarding entity v_3 in Fig. 1, o corresponds to a SQL join-projection operation $v_3 \leftarrow \pi(v_1 \bowtie v_2)$.

Within these pipelines, three types of data entities are involved:

- Source data (SD). The starting point of data flow. Typically, they represent the raw data collected from users or migrated from other data stores.
- Intermediate data (ID). The entities that are the output of the computation process but are not yet ready to be used as a product. They are materialized to enable data reuse and reduce redundant computation.
- Data products (DPs). The final data entities that are ready to be used as products and will not be processed further.

Model data pipelines as a weighted directed cyclic graph (DCG). To model the evolution of data in a structured and traceable manner, we represent the data pipelines using a data lineage [13, 17, 20, 21], a graph-based model that captures how data progresses from its origin to its final form. Specifically, the pipelines are modeled as an edge-weighted directed graph $G = (V, A, w)$, where

- V is a vertex set that denotes the set of data entities, such as SD, ID and DPs. The vertices with out-degree 0 (called *leaves*) represent DPs. The ones with in-degree 0 (called *roots*) represent SD, and the ones with both in-degree and out-degree at least 1 (called *internal vertices*) represent ID.
- A is a directed arc set that represents the transformation flows that produce new data entities from existing ones.
- $w : A \rightarrow [0, 1]$ is a function that assigns a static cost allocation ratio to each arc, as detailed in §3.

Crucially, G is a *cyclic* graph. As discussed in §1, the time-versioned nature of data processing often introduces dependencies on prior temporal snapshots of entities, structurally forming loops. This necessitates the use of a DCG abstraction rather than a DAG.

Other commonly used notations are summarized in Table 2.

Table 2: Notation table.

Notations	Description
$L(G), R(G)$ and $I(G)$	leaves, roots, and internal vertices
$U_G(v)$ (resp., $D_G(v)$)	set of all upstream (resp., downstream) vertices of v
$U_G^1(v)$ (resp., $D_G^1(v)$)	set of all 1-hop upstream (resp., 1-hop downstream) vertices of v
$d_G^+(v)$ (resp., $d_G^-(v)$)	in-degree (resp., out-degree) of v

2.2 Pregel-based Distributed Graph Computation

Our solutions adopt the vertex-centric, distributed Pregel model [32] to support scalable graph-based solution. The Pregel-based paradigm is well-suited for scalable graph-based computation because it decomposes computation into independent vertex actors that maintain local state (*e.g.*, accumulated cost) and exchange information only with neighbors. Our iterative MC calculation algorithm SimpleApp (see §3.3.1) and the algorithm FindFAS (see §4.2.1) for finding an FAS are both implemented using this Pregel-style abstraction to ensure scalability.

Execution proceeds in synchronized iterations called *supersteps*. In each superstep a user-defined `compute()` runs in parallel on every active vertex: it processes incoming messages, updates local state (*e.g.*, adding received cost), and emits messages for delivery in the next superstep. A vertex may call `voteToHalt()` to become inactive and is reactivated if it later receives a message. The job completes when all vertices are inactive and no messages remain in transit.

3 PROBLEM FORMULATION AND BASIC SOLUTIONS

In this section, we formalize the data cost model and the target problem we aim to solve. Then, we present two basic solutions that partially solve the problem.

3.1 Data Cost in Data Pipelines

First, we formalize the cost of manufacturing a data entity v within data pipelines as a structured accumulation of resource expenditures across dependencies.

Direct cost (DC). As stated in §1, the manufacturing of data entities in pipelines is an ongoing process involving periodic recomputation and storage. Consequently, it incurs direct resource fees of CPU usage, memory usage, disk I/O, and storage usage [30, 41, 46, 47]. We define the *direct cost*, denoted as $C_{dc}(v)$, as the total quantified monetary cost incurred *solely* by producing and maintaining v :

$$C_{dc}(v) = C_{CPU}(v) + C_{Mem}(v) + C_{IO}(v) + C_{Sto}(v) \quad (1)$$

where C_{CPU} , C_{Mem} , $C_{IO}(v)$, $C_{Sto}(v)$ denote the monetary cost of quantified resources usage. This represents the fundamental cost injected into the system. The total cost injected into the pipelines is thus $C_{total} = \sum_{v \in V(G)} C_{dc}(v)$.

It is worth noting that the specific composition of $C_{dc}(v)$ is *orthogonal* to our target product costing problem and solutions. Our model is agnostic to the underlying billing schemes and can be flexibly adapted to diverse real-world billing policies [46].

Manufacturing cost (MC). The *manufacturing cost*, denoted as $C_{mc}(v)$, is defined as the total cost of *all* resources consumed in manufacturing entity v across its entire production lineage. It comprises the entity's own direct cost and the inherited costs from its upstream inputs. Formally, for an entity v with upstream inputs $U_G^1(v)$, the manufacturing cost is defined recursively as:

$$C_{mc}(v) = C_{dc}(v) + \sum_{u \in U_G^1(v)} w(u, v) \cdot C_{mc}(u) \quad (2)$$

Here, $w(u, v)$ is the *cost allocation ratio*, representing the fraction of u 's manufacturing cost allocated to v . The second term, $\sum_{u \in U_G^1(v)} w(u, v) \cdot C_{mc}(u)$, represents the *input cost* $C_{ic}(v)$, capturing the cumulative value inherited from direct upstream dependencies.

Cost allocation ratio. Unlike traditional consumption-based costing, our ratio-based strategy is consumption-independent, accommodating the non-rivalrous nature of data. Crucially, to ensure that the total cost of v is fully and precisely distributed across its lineage without duplication (*completeness*, see Theorem 2), we enforce the following conservation property.

DEFINITION 1 (COST CONSERVATION). A data pipeline graph $G = (V, A, w)$ satisfies the *cost conservation property* if the sum of cost allocation ratios for any non-leaf node $u \in V(G) \setminus L(G)$ equals unity:

$$\sum_{v \in D_G^1(u)} w(u, v) = 1$$

This ratio definition is flexible and can be adapted to various allocation strategies, including equal-distribution, usage-based [41, 46], or value-based proxies [9, 22]. For instance, under a usage-based strategy, the weight can be derived from the normalized data volume read by downstream vertices [41]: $w(u, v) = \frac{\text{read_volume}(v \leftarrow u)}{\sum_{k \in D_G^1(u)} \text{read_volume}(k \leftarrow u)}$

where $\text{read_volume}(v \leftarrow u)$ denotes the volume of data read from u to produce v .

Example 1. Consider v_1 , v_2 , and v_3 in Fig. 1. Let $w(v_1, v_3) = 1$, $w(v_2, v_3) = 0.6$, $C_{mc}(v_1) = 3$, $C_{mc}(v_2) = 5$, $C_{dc}(v_3) = 2$, then we have $C_{ic}(v_3) = 1 \times 3 + 0.6 \times 5 = 6$. Thus, $C_{mc}(v_3) = 6 + 2 = 8$.

3.2 Product Costing in Data Pipelines as an MCP Problem

Based on the definition of MC, we demonstrate that the problem of product costing can be reduced to solving an MCP problem.

MC of DPs completely recovers the total cost of the pipelines. The primary goal of product costing is to apportion the total direct cost of the pipelines to the final DPs, with *completeness* guarantee that ensures *all* costs are accounted for *without* duplication. Our crucial observation is that this goal can be achieved by calculating the manufacturing cost, $C_{mc}(p)$, for each DP, as it inherently accumulates all inherited upstream expenditures with its direct cost. We state this property formally below.

THEOREM 2 (COMPLETENESS OF PRODUCT COSTING). Given a data pipeline graph $G = (V, A, w)$ that satisfy the cost conservation property, the total manufacturing cost of data products (leaf nodes) is equal to the total direct cost injected into the system. Formally:

$$\sum_{p \in L(G)} C_{mc}(p) = \sum_{v \in V(G)} C_{dc}(v)$$

The proof is demonstrated in Appendix A¹. Theorem 2 shifts our goal to accurately computing the MC of all DPs, which we term the *calculating the MC of DPs (MCP) problem*.

DEFINITION 2 (THE MCP PROBLEM). Given an edge-weighted DCG $G = (V, A, w)$, a DC vector \mathbf{d} where $d_i = C_{dc}(v_i)$ for all $v_i \in V$, the MCP problem is to compute the MC vector $\mathbf{c}^L \in \mathbb{R}^{|L(G)|}$ such that each c_i^L represents the MC of a leaf node (DP) $p_i \in L(G)$.

Desired goals. We define the desired goals for an algorithm that solves MCP problem as follows.

- **Exactness.** The algorithm must compute the MC $C_{mc}(p)$ for each data product $p \in L(G)$ exactly as defined by the cost model (Eq. 2).
- **Scalability** The algorithm must scale to large data pipelines (e.g., millions of vertices) and complete the computation within a practical time window (e.g., for daily billing cycles).

The necessity of these goals stems from both economic and technical imperatives. First, the exactness of the MCP solution servers as the foundation for the completeness of product costing. It is fundamental to financial accountability, particularly for data pricing and pipeline optimization. Given that cost-based pricing is prevalent in practice [12, 33, 46] and resource optimization is critical, any inaccuracy risks distorting pricing strategies, eroding revenue, and misallocating budgets. Second, scalability is essential for handling enterprise-level data pipelines, which often comprise millions of entities and require timely cost reporting.

¹The complete appendix can be found in the full version of our paper, available at <https://github.com/jerrypl/CostApp>

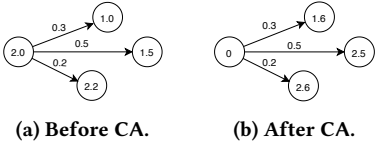


Figure 3: An example of a CA operation.

3.3 Basic Solutions

We present two basic solutions for MCP problem, SimpleApp and MatrixApp. While neither fully satisfies both exactness and scalability goals simultaneously, they serve as fundamental building blocks for our proposed hybrid approach (see §4).

3.3.1 The SimpleApp Algorithm. A straightforward idea to solve MCP problem is to iteratively propagate costs from upstream vertices to downstream ones along the lineage until they fully accumulate at the leaves. Based on this strategy, we introduce SimpleApp, a scalable, vertex-centric algorithm designed to simulate cost propagation along the lineage.

At the heart of SimpleApp is an iterative cost propagation mechanism. It is based on a stateful cost variable $C(v)$ and a cost apportion operation CA that transfers cost states. $C(v)$ represents the cost currently held by v , and initialized with its direct cost *i.e.*, $C(v) \leftarrow C_{dc}(v)$. In each iteration, a cost apportion operation CA is applied to non-leaf vertices to propagate their costs downstream. CA(v) is a two-step state update:

- (1) **Distribute Cost:** For each direct downstream neighbor $v' \in D_G^1(v)$, its cost is updated by adding a proportional share of v 's cost: $C(v') \leftarrow C(v') + w(v, v') \cdot C(v)$.
- (2) **Reset Cost:** The cost at v is set to zero, signifying that its contribution has been fully passed on: $C(v) \leftarrow 0$.

An example of a CA operation is shown in Fig. 3.

Apportion cost via CA Operations based on Pregel. Build upon CA, we introduce SimpleApp that repeatedly applies the CA to all non-leaf vertices to solve MCP problem. We adopt Pregel-based implementation [32] since CA is *vertex centric* and naturally fits distributed graph processing frameworks, enabling a scalable solution.

Algorithm 1: SimpleApp (Pregel-style pseudocode)

```

Input: Graph  $G = (V, A, w)$ , stateful cost variable  $C(v)$ 
Output:  $C^{out}(v)$ 
1 Each vertex  $v \in V$  sets  $C^{out}(v) \leftarrow C(v)$ ;           // Initialization
2 while any non-leaf vertex  $v$  is active do
3   foreach active vertex  $v$  do in parallel
4     /* CA operation in Pregel style
5     compute(msgs)
6       update  $C^{out}(v) \leftarrow C^{out}(v) + \sum_{m_i \in msgs} m_i$ ;
7       sends  $w(v, v') \cdot C^{out}(v)$  to each  $v' \in D_G^1(v)$ ;
8       updates  $C^{out}(v) \leftarrow 0$ ;
9       voteToHalt();
10      // Reactivated upon receiving a message
11
12 return  $C^{out}(v)$ 

```

The algorithm SimpleApp is shown in Alg. 1. It takes input the graph $G = (V, A, w)$, the stateful cost variable $C(v)$. The output is the final cost state $C^{out}(v)$ for all vertices $v \in V$. The algorithm proceeds in supersteps.

Initially, each vertex v initiates a new state $C^{out}(v)$ (line 1). In each superstep, every active non-leaf vertex performs CA operation (line 3). Each vertex collects all incoming costs from the messages received from upstream neighbors and accumulates these into its cost state $C^{out}(v)$ (line 5). SimpleApp then pushes its current cost to its immediate downstream neighbors according to the edge weights (line 6), and resets its cost to zero (line 7), indicating that its cost is “flowed-away”. The process iterates until all non-leaf vertices become in-active. Finally, the algorithm returns the final cost state $C^{out}(v)$ for all $v \in V$ (line 10). The final cost state of DPs c^L can be extracted from $C^{out}(v)$ as $c_i^L \leftarrow C^{out}(p_i)$ for $p \in L(G)$.

SimpleApp is scalable to large graphs due to its Pregel-based distributed parallel computing paradigm [32].

Limitations. For acyclic graphs (DAGs), SimpleApp is guaranteed to terminate and yield exact results (Theorem 3). However, in graphs with cycles (DCGs), costs circulate indefinitely, preventing the algorithm from terminating naturally. While forcing termination via a superstep threshold (see Appendix B) ensures convergence, it inevitably results in approximate solutions, failing the exactness goal.

THEOREM 3. *For any DAG $G = (V, A, w)$ and $C(v)$ initialized as $C_{dc}(v)$, SimpleApp(G, C) terminates and correctly computes the MC vector c^L where $c_i^L = C_{mc}(p_i)$ for all leaves $p_i \in L(G)$ (solve MCP problem) in at most P supersteps, where P is the length of the longest path in G .*

The proof is demonstrated in Appendix C.

3.3.2 The MatrixApp Algorithm. To address the cyclic dependencies where SimpleApp fails, we formulate the problem as a system of linear equations.

Linear System Formulation. As defined in Eq. 2, the manufacturing costs in a cyclic graph are mutually dependent. For each vertex v , its cost is a sum of its direct cost and the apportioned costs from its inputs:

$$C_{mc}(v) - \sum_{u \in U_G^1(v)} w(u, v) \cdot C_{mc}(u) = C_{dc}(v) \quad (3)$$

Considering all vertices $v \in V(G)$ indexed from 1 to n , this forms a global system of $|V(G)|$ linear equations. Let \mathbf{c} be the vector of manufacturing costs $[C_{mc}(v_1), \dots, C_{mc}(v_n)]^T$, \mathbf{d} be the vector of direct costs $[C_{dc}(v_1), \dots, C_{dc}(v_n)]^T$, \mathbf{W} is a *cost allocation matrix* where $\mathbf{W}[i, j] = w(v_i, v_j)$ if there is an arc from v_i to v_j and 0 otherwise, and \mathbf{I} is an identity matrix. The system can be expressed in matrix form (see Appendix D for detailed derivation) as:

$$\mathbf{c} = \mathbf{d} + \mathbf{W}^T \mathbf{c} \quad (4)$$

Solving this system for \mathbf{c} gives a closed-form solution to MCP problem, as shown in Alg. 2.

The invertibility of $(\mathbf{I} - \mathbf{W}^T)$ is guaranteed by the spectral structure of \mathbf{W} : all entries are non-negative, each row sum is at most 1,

Algorithm 2: MatrixApp

Input: Cost allocation matrix \mathbf{W} , DC vector \mathbf{d}
Output: MC vector of DPs \mathbf{c}^L

- 1 Compute $\mathbf{c} \leftarrow (\mathbf{I} - \mathbf{W}^\top)^{-1} \mathbf{d}$;
- 2 Extract the sub-vector \mathbf{c}^L from \mathbf{c} ;
- 3 **return** \mathbf{c}^L

and at least one row sum is strictly less than 1 (the leaves). A formal proof is given in Appendix E.

Limitations. While MatrixApp guarantees exactness by definition, it is computationally prohibitive for large-scale pipelines. Matrix inversion generally incurs cubic time complexity $O(|V|^3)$ and quadratic space complexity $O(|V|^2)$. Even with optimizations for sparse matrices, this approach becomes computationally and memory-prohibitive for pipelines with millions of entities, failing the scalability goal.

In this section, we presented two basic methods for calculating data manufacturing costs. These methods highlight a fundamental trade-off between exactness and scalability, motivating the need for a novel approach that can achieve both goals simultaneously.

4 THE IMPROVED ALGORITHM: COSTAPP

In this section, we introduce CostApp, a novel hybrid algorithm that strategically combines our two basic methods. It delivers an exact, scalable solution for the MCP problem on cyclic graphs.

4.1 Overview of CostApp

The core idea behind CostApp is decoupling and reduction: it transforms an intractable, large-scale problem into an equivalent but easily solvable, compact one. The algorithm CostApp is illustrated in Alg. 3, with a running example shown in Fig. 4. CostApp operates in two main phases:

Phase 1: Acyclic Cost Aggregation. This phase uses scalable, distributed graph algorithms to propagate all direct costs throughout the acyclic portions of the pipelines and consolidate them onto a small, well-defined set of terminal vertices. The process begins by identifying the cyclic dependencies using our scalable FindFAS algorithm (line 1) to obtain an FAS. Instead of simply removing these arcs, we isolate the cycles using GraphEdit (line 2), which replaces each feedback arc with a special path through auxiliary *sink* and *source* vertices. They effectively isolate the cyclic dependency and render the majority of the graph acyclic while preserving cost-flow equivalence, enabling us to use the highly scalable SimpleApp algorithm to efficiently propagate all direct costs (line 5). Upon completion, all costs are precisely aggregated onto a small set of terminal vertices *i.e.*, the original data products and the newly created sink nodes. This sets the stage for an exact solution.

Phase 2: Cyclic Cost Resolution. With all costs consolidated on the terminal vertices, this phase constructs and solves a compact linear system to resolve the remaining cyclic dependencies. First, we extract the aggregated costs from Phase 1 to form a new, reduced direct cost vector \mathbf{d}_{term} (line 6). We then compute the reduced cost allocation matrix, \mathbf{W}_{term} , using GetMatrix (line 7), which captures the cost-flow relationships *only among* these terminal vertices. This

Algorithm 3: CostApp

Input: Graph $G = (V, A, w)$, initial cost state $C(v) = C_{dc}(v)$ for all $v \in V$
Output: The MC vector of DPs \mathbf{c}^L

/* Phase 1: Acyclic Cost Aggregation */

- 1 $A_{\text{FAS}} \leftarrow \text{FindFAS}(G)$; // (1.a) Identifying cycles
- 2 $(G_1, V_{sk}, V_{sr}) \leftarrow \text{GraphEdit}(G, A_{\text{FAS}})$; // (1.b) Isolating cycles
- 3 Let G_{DAG} be the subgraph of G_1 without sink-to-source arcs;
- 4 Let V_{term} be the set of terminal vertices, comprising the leaves of G_{DAG} , *i.e.*, $L(G) \cup V_{sk}$;
- 5 $C_1 \leftarrow \text{SimpleApp}(G_{\text{DAG}}, C)$; // (1.c) Aggregating costs
- 6 $\mathbf{d}_{\text{term}} \leftarrow \text{ExtractCosts}(C_1, V_{\text{term}})$;
- 7 $\mathbf{W}_{\text{term}} \leftarrow \text{GetMatrix}(G_{\text{DAG}}, V_{sk}, L(G))$; // (2.a) Getting the cost allocation matrix
- 8 $\mathbf{c}^L \leftarrow \text{MatrixApp}^*(\mathbf{W}_{\text{term}}, \mathbf{d}_{\text{term}})$; // (2.b) Solving a compact system for final costs
- 9 **return** \mathbf{c}^L

transforms the original large-scale problem into a compact and equivalent linear system, which we solve exactly and efficiently using MatrixApp* (a variant of MatrixApp, see §4.3.3) (line 8). This final step yields the true manufacturing costs for all DPs, accurately accounting for the complex cyclic flows isolated in Phase 1.

Our crucial design is the injection of sink vertices and source vertices on the feedback arcs. To overcomes the *cyclic* and *massive scale* challenges (stated in §1), we introduce sink vertices that acts as *collectors* to intercept all cost that would have flowed over feedback arcs. This enable us to simultaneously *isolate cycles* and *simplifies the cost flow dependencies* in Phase 1. To model the reduced compact system, source vertices are introduced to serve as *re-injection points*. It allow us to capture how the aggregated cost at sink vertices would re-entered the original the graph, based on which we can efficiently solve the reduced linear system in Phase 2.

By strategically injecting auxiliary vertices and combining SimpleApp and MatrixApp, CostApp shifts the computational bottleneck from inverting a massive $|V| \times |V|$ matrix to inverting a tiny one (often less than 0.1% of $|V|$ in size). Our design is simple yet effective, achieving a dramatic performance gain while preserving result exactness. We now detail each phase.

4.2 Phase 1: Acyclic Cost Aggregation

The goal of the phase 1 is to aggregate all direct costs $C_{dc}(v)$ from millions of internal vertices onto a small set of terminal vertices, while preserving the manufacturing cost of every DP. To achieve this, directly using SimpleApp on the original graph to push cost would fail, as costs would circulate indefinitely in cycles. Our solution, therefore, involves three steps: (1) identifying cycles via finding an FAS, (2) isolating cycles via graph editing, and (3) aggregating costs on the resulting acyclic graph.

4.2.1 1. Identifying Cycles via Finding an FAS. To make cost aggregation possible, we must first break all cycles while preserving the major of the original graph structure. A standard way in graph theory is to find a FAS, *i.e.*, a subset of arcs whose removal makes the graph acyclic. While finding a minimum FAS is an NP-hard

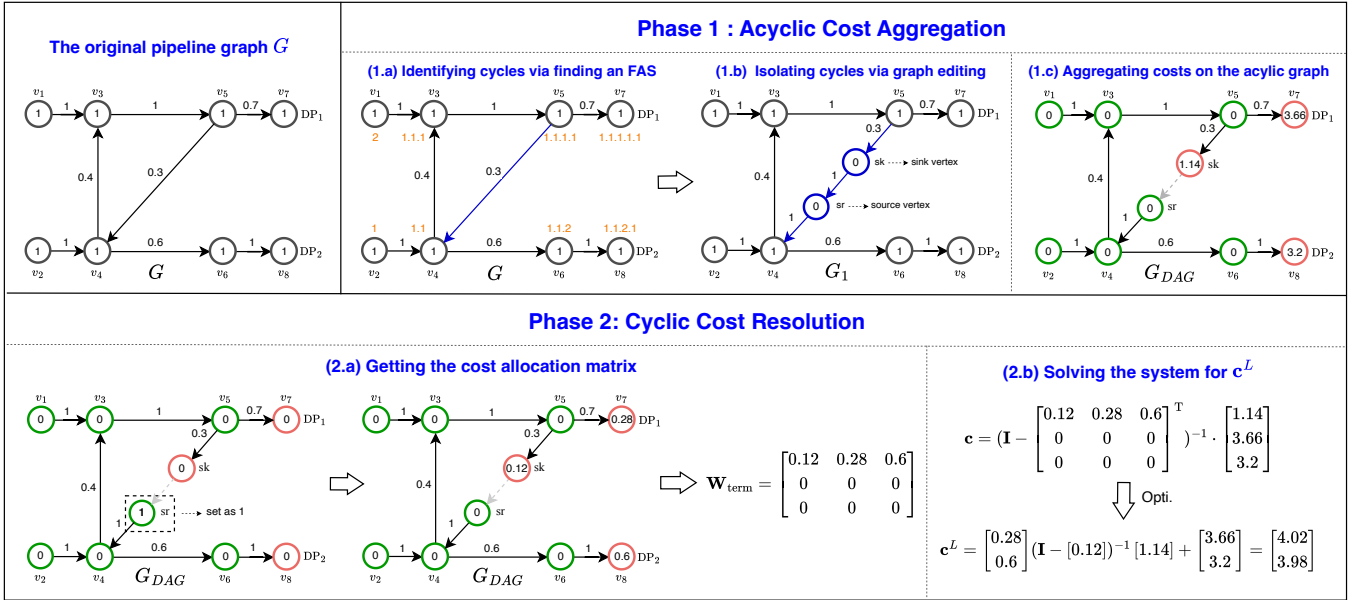


Figure 4: An illustrative workflow of CostApp. Initial cost state of each vertex is set to 1 for better illustration. (1.a) Ordering labels (orange) from Label identify the feedback arc (blue). (1.b) New sink/source vertices (blue) are inserted to isolate the cycle. (1.c) SimpleApp aggregates costs onto terminal vertices (red), leaving the remaining vertices (green) with zero cost. (2.a) Unit costs are injected at source vertices to derive W_{term} . (2.b) MatrixApp solves the reduced linear system to yield exact MCs.

problem [16, 18, 25], but for our purpose *any* valid FAS suffices, as long as it can be computed efficiently on large graphs.

We therefore design a scalable Pregel-style algorithm FindFAS with the following high-level strategy. First, we establish a linear ordering over all vertices by assigning each vertex a hierarchical label. Given this ordering, any arc $\langle u, v \rangle$ that goes *backward* (*i.e.*, the label of u is larger than that of v) is classified as a feedback arc. The set of all such arcs forms a valid FAS.

Our strategy is to first establish a linear ordering of all vertices in the graph G . Given such an ordering, any arc $\langle u, v \rangle$ where u appears after v is considered a *backward* or inconsistent arc. The set of all such inconsistent arcs constitutes a valid FAS. Based on this strategy, we devise a distributed labeling algorithm to generate this ordering, followed by a simple check to identify the inconsistent arcs.

Distributed labeling for vertex ordering. To construct the ordering, we use a synchronous labeling algorithm Label. Each vertex v maintains a label $Label(v)$, represented as a dot-separated sequence of positive integers (*e.g.*, ‘1.2.1’). The labels induce a lexicographic order $>_{lo}$ (Definition 3).

DEFINITION 3 (LEXICOGRAPHICAL LABEL ORDERING). *Given two distinct labels $Label_A = a_1.a_2.\dots.a_p$ and $Label_B = b_1.b_2.\dots.b_q$, we say $Label_A$ is lexicographically greater than $Label_B$, denoted $Label_A >_{lo} Label_B$, if either:*

- (1) *$Label_A$ is a prefix of $Label_B$ (*i.e.*, $p < q$ and $a_i = b_i$ for all $1 \leq i \leq p$).*
- (2) *There exists an index $k \leq \min(p, q)$ such that $a_i = b_i$ for all $i < k$ and $a_k < b_k$.*

The algorithm Label is designed based on Pregel to support large graph. It starts by assigning distinct integer labels to all roots (vertices with in-degree 0). In each superstep, every active vertex v :

- (1) collects labels from its upstream neighbors,
- (2) adopts the lexicographically largest incoming label if it is greater than $Label(v)$, and
- (3) propagates an extended version of its new label (by appending a suffix) to its downstream neighbors.

This process repeats until no vertex updates its label. The full Pregel-style pseudocode is given in Appendix F. With each vertex labeled, we can classify arcs and identify an FAS.

THEOREM 4. *Label terminates and assigns a stable label to every vertex in at most $L_p + 1$ supersteps, where L_p is the length of the longest simple path in G .*

Finding an FAS. Once Label terminates, every arc $\langle u, v \rangle$ falls into exactly one of the following types:

- (1) direct forward arc: $Label(u)$ is a prefix of $Label(v)$ (*e.g.*, $Label(v_4) = 1.1$, $Label(v_6) = 1.1.2$ in Fig. 4);
- (2) cross forward arc: $Label(u) >_{lo} Label(v)$ but $Label(u)$ is not a prefix of $Label(v)$;
- (3) feedback arc: $Label(v)$ is a prefix of $Label(u)$ (*e.g.*, $Label(v_5) = 1.1.1.1$, $Label(v_4) = 1.1$ in Fig. 4).
- (4) cross backward arc: $Label(v) >_{lo} Label(u)$ but $Label(v)$ is not a prefix of $Label(u)$ (*e.g.*, $Label(v_1) = 2$, $Label(v_3) = 1.1.1$ in Fig. 4).

The set of all arcs satisfying condition (3) constitutes FAS *i.e.*, AFAS. Intuitively, after removing AFAS, every remaining edge follows the label order, so any directed path must follow a strictly increasing sequence of labels and thus cannot form a cycle.

LEMMA 1. *The set $A_{\text{FAS}} = \{(u, v) \in A(G) \mid \text{Label}(v) >_{lo} \text{Label}(u)\}$ is a valid feedback arc set for G .*

The proof is in Appendix G.

Therefore, the overall FindFAS procedure first runs Label and then, in a single superstep, lets each vertex inspect its incoming arcs and mark those with $\text{Label}(u) >_{lo} \text{Label}(v)$ as feedback arcs. Its superstep complexity is therefore $O(L_p)$, dominated by Label.

An illustration of FindFAS is shown in Fig. 4 (1.a), each vertex is assigned a hierarchical label (highlighted in orange) by calling Label (*e.g.*, v_4 gets ‘1.1’). Then, arcs that point backward according to these labels are identified as feedback arcs (highlighted in blue, *e.g.*, (v_5, v_4) where $\text{Label}(v_4) >_{lo} \text{Label}(v_5)$).

4.2.2 Isolating Cycles via Graph Editing. To isolate cyclic dependencies, simply deleting the FAS arcs would distort the true dependencies and lead to incorrect cost calculations. Instead, our goal is to *isolate* the cyclic dependencies while preserving the cost-flow behavior seen from the original vertices, and at the same time create explicit *entry* and *exit* points that allow us to aggregate and later resolve the cyclic costs.

To this end, we introduce a graph transformation GraphEdit. For each feedback arc $(u, v) \in A_{\text{FAS}}$, GraphEdit performs the following local rewrite on G :

- Remove the original arc (u, v) .
- Create two new auxiliary vertices: a *sink* vertex v_{sk} and a *source* vertex v_{sr} , and add them to V_{sk} and V_{sr} , respectively.
- Insert three arcs forming the path $u \rightarrow v_{sk} \rightarrow v_{sr} \rightarrow v$: (u, v_{sk}) with weight $w(u, v)$, and (v_{sk}, v_{sr}) , (v_{sr}, v) both with weight 1.

An illustration of this transformation is shown in Fig. 4(1.b). The feedback arc (v_5, v_4) is replaced by the path $v_5 \rightarrow v_{sk} \rightarrow v_{sr} \rightarrow v_4$, where v_{sk} and v_{sr} are newly created sink and source vertices, respectively. Intuitively, v_{sk} acts as a *collector*: it intercepts all cost that would have flowed from u into the cycle through (u, v) , allowing Phase 1 to aggregate such *cycle-bound* cost onto a small set of sink vertices. Symmetrically, v_{sr} serves as a *re-injection point*: in Phase 2, it enables us to model how the aggregated cost at v_{sk} would have re-entered the original downstream part of the graph, via a reduced cost allocation matrix \mathbf{W}_{term} . A formulation of GraphEdit is illustrated in Appendix H.

Crucially, this transformation does not change the manufacturing cost of any original vertex. The path $u \rightarrow v$ in G is replaced by an equivalent path $u \rightarrow v_{sk} \rightarrow v_{sr} \rightarrow v$ in G_1 that carries exactly the same cost (up to the introduced auxiliary vertices), and all other edges remain untouched. As a result, from the perspective of the original vertices, the total cost transmitted along every path is preserved. This is formalized below.

THEOREM 5 (EQUIVALENCE OF MC OF DPs AFTER GRAPH EDITING). *Let G_1 be the graph produced by applying GraphEdit to a graph G with a feedback arc set AFAS. The manufacturing cost $C_{\text{mc}}(p)$ for any original data product $p \in L(G)$ is identical in both the original system defined on G and the transformed system defined on G_1 .*

The proof is provided in Appendix I.

4.2.3 Aggregating Costs on the Acyclic Graph. After graph editing, we obtain a modified graph G_1 with additional sink/source vertices and arcs. Let A_{SS} denote the set of sink-to-source arcs $\{(v_{sk}, v_{sr})\}$. By construction, removing A_{SS} yields an acyclic subgraph $G_{\text{DAG}} = G_1 \setminus A_{SS}$. The leaves of G_{DAG} , which we call *terminal vertices*, are

$$V_{\text{term}} = L(G_{\text{DAG}}) = L(G) \cup V_{sk},$$

that is, all original DPs (leaves of G) and all newly created sink vertices.

The acyclic structure of G_{DAG} allows us to apply the scalable SimpleApp algorithm to propagate costs exactly. We run SimpleApp on G_{DAG} (Alg. 3, line 3), initializing each vertex v with its direct cost $C_{dc}(v)$. By Theorem 3, this process terminates in at most P supersteps, where P is the length of the longest path in G_{DAG} , and correctly transfers all costs to the leaves of G_{DAG} , *i.e.*, to V_{term} .

Let C_1 denote the resulting cost state. It satisfies a crucial property:

- For every terminal vertex $t \in V_{\text{term}}$, $C_1(t) > 0$ in general;
- For every non-terminal vertex $v \in V(G_1) \setminus V_{\text{term}}$, $C_1(v) = 0$.

As illustrated in Fig. 4(1.c), the entire initial direct cost of the pipeline has now been losslessly consolidated onto the much smaller terminal set $V_{\text{term}} = \{v_7, v_8, v_{sk}\}$ (highlighted in red). In other words, Phase 1 has used a scalable graph algorithm to transform a large, distributed MCP instance into a compact representation over a small number of terminal vertices, thereby setting up Phase 2 to resolve the remaining cyclic dependencies via a tiny linear system.

4.3 Phase 2: Cyclic Cost Resolution

Phase 1 has effectively consolidated the entire pipeline’s direct costs onto the terminal vertices V_{term} . Consequently, MCP problem is reduced to determining how the aggregated costs at the sink vertices V_{sk} are redistributed among themselves and ultimately to the data products $L(G)$. This redistribution is governed by the feedback relationships isolated in the $v_{sk} \rightarrow v_{sr}$ paths, which we now resolve as a compact linear system.

4.3.1 Formulating the Reduced Linear System. To formulate the reduced system that only includes V_{term} , our key insight is that we can treat the aggregated costs C_1 on V_{term} as *new* direct costs for this reduced system. We denote this reduced cost vector by \mathbf{d}_{term} , where each entry corresponds to $C_1(v)$ for a terminal vertex v in V_{term} . Consequently, this reduced system follows our original cost definition for their final manufacturing costs, \mathbf{c}_{term} (Eq. 2):

$$\mathbf{c}_{\text{term}} = \mathbf{d}_{\text{term}} + \mathbf{W}_{\text{term}}^T \mathbf{c}_{\text{term}} \quad (5)$$

Here, \mathbf{c}_{term} is the vector of final manufacturing costs for the terminal vertices, and \mathbf{W}_{term} is a reduced cost allocation matrix that captures how cost flows *among* these terminal vertices via the isolated cyclic dependencies.

This equation has exactly the same form as the system defined in §3.3.2, and \mathbf{W}_{term} inherits the same non-negativity and row-sum properties as \mathbf{W} . Therefore, $(\mathbf{I} - \mathbf{W}_{\text{term}}^T)$ is invertible and the reduced system has a unique solution (proved in Appendix E). It allows us to solve this system using MatrixApp to get \mathbf{c}_{term} and thus MCP problem be solved exactly.

Since \mathbf{d}_{term} is already determined by Phase 1 (from C_1 in §4.2.3), the remaining challenge in Phase 2 is to compute the reduced allocation matrix \mathbf{W}_{term} . We describe how to do this efficiently by leveraging source vertices in the next step.

4.3.2 Getting the Cost Allocation Matrix. The remaining task in Phase 2 is to construct the reduced cost allocation matrix \mathbf{W}_{term} . This matrix captures the cost-flow relationships *among* terminal vertices, *i.e.*, an entry $\mathbf{W}_{\text{term}}[i, j]$ represents the fraction of cost that flows from terminal vertex t_i to t_j .

Recall that $V_{\text{term}} = L(G) \cup V_{sk}$ and that every sink $v_{sk} \in V_{sk}$ has a corresponding source vertex $v_{sr} \in V_{sr}$ connected by a sink-to-source arc. Our crucial observation is that for a sink vertex t_i , $\mathbf{W}_{\text{term}}[i, j]$ is equivalent to the cost received by terminal vertex t_j when a *unit cost* is injected at the corresponding source vertex v_{sr} and allowed to traverse the acyclic graph G_{DAG} . This is because the only way for cost to flow from t_i to other terminal vertices in G_1 is through the path $t_i \rightarrow v_{sr} \rightarrow \dots \rightarrow t_j$. This observation allow us to compute \mathbf{W}_{term} efficiently using SimpleApp by injecting unit cost to each source vertex.

Based on this idea, we design GetMatrix to compute \mathbf{W}_{term} efficiently based on Pregel, as illustrated in Alg.11. To eable efficient computation within single Pregel job, we adopt a *map-based* cost propagation approach. Specifically, instead of a scalar cost, we assign a cost state map to each vertex (lines 3) to record {vertex: cost} pair. We inject unit costs at all source vertices (lines 4-6) and propagate them through G_{DAG} using SimpleApp* (line 7). Due to the cost conservation property (Definition 1), the final cost state map at any terminal vertex t_i constitutes the i -th column of \mathbf{W}_{term} (lines 8-11). Thus, all columns of \mathbf{W}_{term} are obtained in a *single* Pregel job, setting the stage for solving the reduced system in the next step.

Note that this map-based approach rely on a variant of SimpleApp that can aggregate cost maps by summing values of same keys. We term this variant SimpleApp* and provide its Pregel-style pseudocode in Appendix J. Noting that GetMatrix (line 8 in Alg.3) and SimpleApp (line 6 in Alg.3) both operate with Pregel on G_{DAG} , they can be merged into a single Pregel workload to avoid duplicated overhead. We denote this merged workload as S&G in the following parts.

4.3.3 Solving the Reduced Linear System. With \mathbf{W}_{term} and \mathbf{d}_{term} in hand, we can solve MCP problem by invoking MatrixApp to solve the compact linear system defined in §4.3.1. Instead of naively inverting the full matrix \mathbf{W}_{term} , we exploit the topological structure of V_{term} to further reduce the computational cost.

Recall that $V_{\text{term}} = L(G) \cup V_{sk}$. Since data products are leaves in the global graph, they do not propagate costs. Consequently, the reduced allocation matrix \mathbf{W}_{term} is *block upper triangular*:

$$\mathbf{W}_{\text{term}} = \begin{bmatrix} \mathbf{W}_{sk,sk} & \mathbf{W}_{sk,dp} \\ \mathbf{0} & \mathbf{0} \end{bmatrix}.$$

This structure allows us to solve the system and obtain the final MC of DPs by computing:

$$\mathbf{c}_{dp} = \mathbf{d}_{dp} + \mathbf{W}_{sk,dp}^T (\mathbf{I}_{sk} - \mathbf{W}_{sk,sk}^T)^{-1} \mathbf{d}_{sk}$$

Algorithm 4: GetMatrix

```

Input: Graph  $G_{DAG} = (V, A, w)$ , set of sink vertices  $V_{sk}$ , data
products  $L(G)$ .
Output: Cost allocation matrix  $\mathbf{W}_{\text{term}} \in \mathbb{R}^{k \times k}$ 
/* 1. Setup and Initialization */
1 Let  $V_{\text{term}} = L(G) \cup V_{sk}$ ,  $k = |V_{\text{term}}|$ ,  $m = |V_{sr}|$ ;
2 Initialize  $\mathbf{W}_{\text{term}}$  as a  $k \times k$  zero matrix;
3  $C(v) \leftarrow$  empty map  $\emptyset$  for each  $v$ ; // Initiates a cost state map
4 for  $i \leftarrow 1$  to  $m$  do
5   Let  $v_{sr,i}$  be the  $i$ -th source vertex;
6    $C(v_{sr,i}) \leftarrow \{i : 1\}$ ; // Inject a unit cost
/* 2. SimpleApp* aggregates maps by summing values of same keys */
7  $C^{out} \leftarrow \text{SimpleApp}^*(G_{DAG}, C)$ 
/* 3. Fill the matrix with the results */
8 for  $i \leftarrow 1$  to  $k$  do
9   Let  $t_i$  be the  $i$ -th terminal vertex;
10  for  $j \leftarrow 1$  to  $m$  do
11     $\mathbf{W}_{\text{term}}[j, i] \leftarrow C^{out}(t_i).\text{getValue}(j, 0)$ ; // Get value for
      source index  $i$ , default to 0 if missing
12 return  $\mathbf{W}_{\text{term}}$ 

```

where \mathbf{d}_{dp} and \mathbf{d}_{sk} are the subvectors of \mathbf{d}_{term} corresponding to data products and sink vertices, respectively. We term this variant as MatrixApp*.

This optimization further reduces the dominant inversion cost to $O(|V_{sk}|^3)$, followed by a cheaper matrix-vector multiplication. In typical data pipelines, the number of sink arcs (equals the number of feedback arcs) is vastly smaller than the total number of vertices ($|V_{sk}| \ll |V(G)|$). The exactness of CostApp is preserved due to Theorems 5, 3 and the correctness of MatrixApp.

4.4 Efficiency Analysis

The efficiency of CostApp is rooted in its hybrid design, which transforms a computationally intractable problem into a compact one while preserving exactness. By strategically isolating cyclic dependencies, it leverages the strengths of both distributed graph processing and solving linear system. Tab. 3 summarizes the efficiency and complexity comparison of the algorithms.

Table 3: Complexity comparison.

Category	Algorithm / Module	Scalability	Exactness	Time Complexity
Baselines	MatrixApp SimpleApp	Low High	Exact Approximate	$O(V ^3)$ $O(S \cdot (V + A))$
	CostApp	High	Exact	$O(L_p \cdot (V + A) + A_{FAS} ^3)$
Ours	FindFAS S&G (SimpleApp + GetMatrix) MatrixApp*	- - -	- - -	$O(L_p \cdot (V + A))$ $O(L'_p \cdot (V + A))$ $O(A_{FAS} ^3)$

Notation: $|V|$ is the number of vertices, $|A|$ is the number of arcs, $|A_{FAS}|$ is the size of the feedback arc set, S is the number of supersteps (determined by configured accuracy-runtime trade-off, see §5.2.1). $L_p \approx L'_p$ are the longest path length of G, G_{DAG} , respectively.

As shown in Tab. 3, the total complexity of CostApp is the sum of its distributed and centralized components: $O(L_p \cdot (|V| + |A|)) + O(|A_{FAS}|^3)$. The first term, $O(L_p \cdot (|V| + |A|))$, represents the near-linear complexity of the Pregel-based modules (FindFAS, S&G). These steps handle the bulk of the computation and dominate the overall runtime. The second term, $O(|A_{FAS}|^3)$, is the cost of the final MatrixApp*. The core innovation of CostApp is reducing the

dimension of this problem from $|V|$ to $|A_{FAS}|$. Since the number of feedback arcs is typically vastly smaller than the total number of vertices ($|A_{FAS}| \ll |V|$).

5 EXPERIMENTS

In this section, we conduct a comprehensive experimental evaluation of our proposed CostApp for MCP problem. Our goal is to answer the following research questions:

- **RQ1: Exactness and Scalability.** How CostApp outperform baselines in terms of exactness and scalability?
- **RQ2: Modular Evaluation.** What are the performance characteristics of CostApp’s individual components, and where are the primary computational bottlenecks?
- **RQ3: Real-world Efficiency.** How effective and practical is CostApp when applied to large-scale, real-world data pipelines?

5.1 Experimental Setup

Our distributed tasks, including Pregel-based graph computations and SQL queries, are conducted on MaxCompute platform [11] that deployed on production clusters at Alibaba. The matrix related operations including MatrixApp are performed on a single machine because distributed executed matrix inversion suffers from prohibitive communication overhead, complex synchronization requirements [14] and challenging deployment on general-purpose distributed platforms [34]. Consequently, our approach is designed to avoid prohibitive execution of matrix inversion rather than brute-force it in a distributed manner. The concrete settings are shown in Table 4. Unless otherwise specified, all tasks are executed based on the setting in Table 4. We denote S&G as the combination of SimpleApp and GetMatrix modules in CostApp (lines 5-6 in Alg. 3). MatrixApp* denotes the linear system solver consisted in CostApp (line 8 in Alg. 3).

Table 4: Execution form of modules of CostApp (Alg. 3) and the setting of platforms.

Modules	Execution form	Pregel/SQL	[workers]	100
FindFAS	Pregel		memory per worker	30GB
GraphEdit	SQL		[threads] per worker	1
S&G	Pregel		[cpu cores] per worker	8
MatrixApp*	Single Machine	Single Machine	memory	100GB
			[cpu cores]	8

(a) Execution form of modules.

(b) Platform settings.

Baselines. Since our work represents the *first* effort to perform product costing in data pipelines and solve the unique challenges therein, we compare CostApp against our two basic solutions in §3.3, which are directly apply SimpleApp and MatrixApp to the original graph G .

Datasets. We use both real-world and synthetic datasets.

Real-world Datasets: We use four large-scale production data pipeline graphs from Alibaba, anonymized as G1–G4. Their detailed statistics are presented in Table 5. The network is scale-free and the degree of each node in these graph follows a power-law distribution, with an average degree of each entity 2.5. A graphic view of the degree distribution is shown in Fig. 5. We open source these datasets and they represents the first publicly available real-world

	#Vertices	#Arcs	#DPs
G1	28,181,925	66,758,378	10,003,135
G2	11,061,395	36,345,530	5,805,784
G3	712,772	3,808,320	309,852
G4	581,853	3,341,002	252,812

Table 5: Statistics of experimental graphs.

data pipeline graphs in data-insetive enterprises, to the best of our knowledge.

Synthetic Datasets: To systematically evaluate performance under controlled conditions, we use synthetic graphs with varying parameters, including number of vertices ($|V|$), edge density (average degree), and the number of injected cycles. To simulate the degree distribution of the scale-free real-world datasets (as in Fig. 5), the graph was generated using a Barabási–Albert model [10]. Unless otherwise specified, $|V| = 10^6$ and $|A| = 3|V|$ to simulate the scale and density of real-world pipelines.

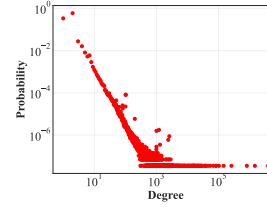


Figure 5: Degree distribution

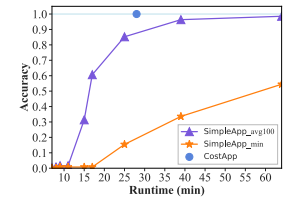


Figure 6: Exactness evaluation on G1.

5.2 Exactness and Scalability

To answer RQ1, we evaluate the exactness and scalability of CostApp compared to the basic solutions.

5.2.1 Exactness. Fig. 6 presents the outperforming exactness of CostApp and the accuracy-runtime trade-off of SimpleApp. CostApp achieves perfect accuracy (1.0) in approximately 28 minutes, delivering a guaranteed, exact cost result for all DPs. In contrast, the iterative baseline SimpleApp exhibits shortfalls. While the average accuracy of the 100 worst-performing data products (SimpleApp_avg100) appears to converge, the minimum accuracy (SimpleApp_min) remains critically low, reaching only 0.55 even after 60 minutes. This discrepancy highlights the unreliability of approximate methods for financial applications such as product costing.

5.2.2 Scalability. We now evaluate the scalability of CostApp by analyzing the runtime performance with respect to various graph characteristics, including the number of vertices, edge density, and the number of cycles. The result is shown in Fig. 7.

Figure 7(a) demonstrates the scalability advantage of CostApp. While the baseline MatrixApp fails on graphs exceeding 10^4 vertices due to its cubic complexity, CostApp exhibits near-linear scalability, successfully processing graphs with 10^7 vertices. Similarly, its runtime scales linearly with the number of arcs ($|A|$), as shown in Figure 7(b), consistent with the communication complexity of the distributed graph-processing stages.

Figure 7(c) isolates the impact of cyclic complexity. It reveals that the total runtime of CostApp increases with the size of the feedback arc set ($|A_{FAS}|$). Crucially, the growth curve of the total

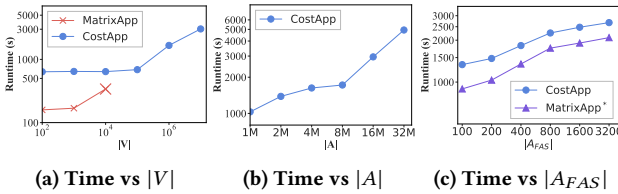


Figure 7: Comparison of scalability of algorithms.

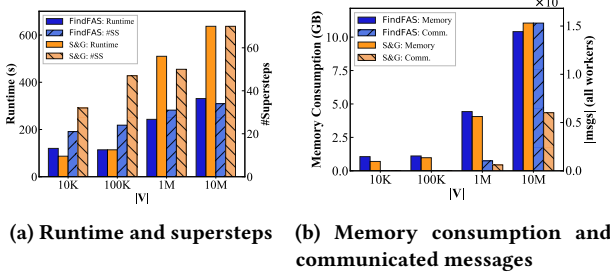


Figure 8: Evaluation of Pregel-based modules under varying $|V|$.

runtime parallels that of the MatrixApp* component. This indicates that the distributed graph-processing stages (represented by the gap between the two curves) impose a relatively constant overhead, while the marginal increase in runtime is primarily driven by the matrix operations. This result validates our hybrid design, which successfully isolates the computationally intensive, cycle-dependent workload into a compact algebraic step.

5.3 Modular Evaluation

To answer RQ2, we profile the main components of CostApp.

Pregel-based modules. Fig. 8 presents the performance characteristics of the core Pregel-based modules of CostApp: the cycle-finding algorithm FindFAS and the S&G module.

As shown in Fig. 8a, the runtime of both modules demonstrates near-linear scalability and moderate growth with the number of vertices ($|V|$). The S&G module, which executes map-based graph traversals for cost state propagation, consistently exhibits almost double the execution time of FindFAS. Furthermore, the number of supersteps correlates strongly with the runtime growth. This confirms that the number of supersteps dominates the overall runtime, a characteristic feature of Pregel-like systems [32].

Fig. 8b details the resource consumption. Memory usage scales predictably with graph size, remaining within 12GB per worker for 10^7 vertices. The FindFAS module is more communication-intensive in terms of message count due to label propagation across the cyclic graph. In contrast, S&G generates significantly fewer messages (less than half when $|V| = 10^7$) since it operates on the DAG. However, S&G employs a map-based mechanism that consumes higher computation and communication bandwidth per message. Consequently, the overall runtime of S&G is almost double that of FindFAS.

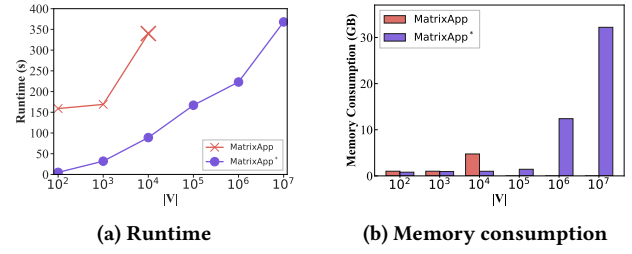


Figure 9: Performance comparison of MatrixApp and MatrixApp*.

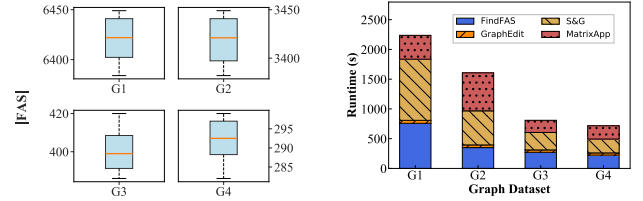


Figure 10: Sizes of FAS on G1–G4.

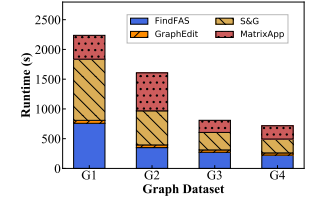


Figure 11: Overall evaluation on G1–G4 and time breakdown.

Linear system solver MatrixApp*. Fig. 9a illustrates the performance gains of our hybrid approach in handling the matrix inversion task. The baseline MatrixApp exhibits runtime that grows cubically with the graph size $|V|$, becoming computationally prohibitive for graphs exceeding 10^4 vertices. This is because the dominate memory cost of matrix inversion in MatrixApp grows quadratically with $|V|$, leading to excessive memory pressure and eventual out-of-memory failures on large graphs (see Fig. 9b). In contrast, the runtime of MatrixApp* (the solver component within CostApp) is faster (at least 2.8x outperforming) and scales gracefully to graphs with 10^7 vertices. Fig. 9b further reveals that MatrixApp* maintains a lower memory footprint at the same level of graph size, reducing the memory pressure and allowing execution on graphs of tens of millions sizes with reasonable memory resources. This performance improvement is a direct result of our dimensionality reduction strategy that transforms the intractable problem of inverting a massive matrix into an efficient inversion of a tiny matrix whose size is determined by the feedback arc set (e.g., for the case of $|V| = 10^6$, $|AFAS| = 312 \ll |V|$). This result confirms that the primary computational bottleneck of direct algebraic solutions is effectively eliminated.

5.4 Real-world Pipeline Evaluation

To validate the performance of CostApp (RQ3) on practical pipeline graphs, we conducted experiments on four large-scale data pipelines from production systems at Alibaba. These graphs, anonymized as G1–G4, represent diverse and complex data pipeline workflows.

Sizes of FAS. As the size of FAS identified by FindFAS directly impacts the efficiency of following steps, we first evaluate its effectiveness. Fig. 10 shows the size of FAS under real-word graphs G1–G4. We observe that FindFAS output a random size of FAS that is around 1% to 3% of $|A|$. The result shows a bit of randomness but remains relatively stable across different runs, indicating the

robustness of FindFAS. This small size of FAS is crucial for ensuring the efficiency of the subsequent matrix inversion step.

Overall Performance and Breakdown. We evaluate the performance and scalability of CostApp on four large-scale production data pipelines from Alibaba, anonymized as G1-G4, with results shown in Fig. 11.

The empirical results demonstrate the practical efficiency of CostApp on industrial-scale graphs. On the largest graph, G1, the end-to-end execution completes in approximately 2250 seconds (under 38 minutes), a runtime that comfortably fits within typical daily batch-processing windows. As the graph size decreases from G1 to G4, the total runtime scales down gracefully, confirming the algorithm’s scalability.

A breakdown of the execution time reveals the performance characteristics of CostApp’s components. The distributed graph processing stages, FindFAS and S&G, constitute the primary computational workload, jointly accounting for over 80% of the total runtime on G1. The GraphEdit step, which performs a simple graph transformation, has a negligible cost across all datasets, consistently taking less than 1% of the total time. The runtime of the MatrixApp* remains a small and manageable fraction of the total execution time. While its relative contribution appears to increase on smaller graphs (from 18% on G1 to 33% on G4), its absolute time decreases significantly.

Overall, experimental results demonstrate that our approach achieves both exactness and scale to massive data pipelines. CostApp can be completed within 1 hour on graphs of Alibaba’s real pipeline with millions of vertices, making it suitable for time-sensitive scenarios (e.g., , daily billing).

6 RELATED WORKS

6.1 Data Pipelines

Data pipelines, particularly ETL (Extract-Transform-Load) workflows, have been widely studied as the backbone of data warehousing and analytics [8]. They enable the automated extraction of data from diverse sources, support complex transformations to ensure data quality and consistency, and facilitate loading into target stores for subsequent analysis or selling. Many big companies embrace data pipelines to build data manufacturing lines and provide business data pipeline platforms, e.g., Microsoft Dataflow [6], AWS Data Pipeline [7], Google Cloud Dataflow [5], Apache Airflow [3] etc. A typical data pipeline is executed in scheduled batch mode [35], which improves efficiency by processing large volumes of data together, which minimizes the load on source systems by operating during off-peak hours. At the same time, a real-time pipeline aims to improve latency and provide more timely data results.

6.2 Cost of Digital Product in Economy

The cost structure of digital products differs fundamentally from that of physical goods, due to major reductions in search, replication, transportation, tracking, and production costs [37]. Search and transportation are made efficient by the Internet, enabling easy discovery and access. Replication costs approach zero, allowing scale, customization, and new models such as bundling and subscriptions [31, 39]. Low tracking costs facilitate personalized pricing, while

raising concerns about privacy [19, 36]. Due to free-duplication nature of data, the production cost of data only contains fixed cost that is not related to the sharing amount. Thus, the unit production cost can approaches zero through sharing as long as sufficient reuse and sales volume. These facilitate the development of innovative pricing strategies and the evolution of data marketplaces [28, 38, 47]. Different from prior works that focus on the cost structure and pricing strategies of digital products, our work aims to product costing in data pipelines, which is orthogonal to cost structure and a prerequisite for pricing.

7 CONCLUSION AND FUTURE WORK

In this paper, we addressed the critical challenge of product costing in large-scale data pipelines. We formalized the MCP problem to account for the non-rivalrous nature of data. To solve this, we proposed CostApp, a hybrid algorithm that synergizes distributed graph processing with matrix inversion. By strategically isolating cyclic dependencies via a feedback arc set, CostApp reduces the computational complexity of exact costing from cubic to near-linear relative to the graph size. Extensive experiments on real-world production pipelines at Alibaba demonstrate that our approach achieves both result exactness and high scalability.

Future work. We present some directions to inspire future work. (1) *Explainable product costing in data pipelines.* For fine-grained cost optimization, enterprises require a detailed understanding of how each upstream data entity contributes to the cost of a final data product. This can be achieved by maintaining a map that tracks the propagation of monetary costs from each component through the pipeline. This method yields a detailed breakdown of each data product, attributing its total cost to its constituent components and enabling explainability. This idea will incur additional storage and communication overhead. We leave the concrete design and optimization of solutions to this explainability as future work.

(2) *Exploration of potential applications of CostApp.* Although motivated by data pipelines, CostApp’s core capability, which is solving large-scale sparse linear systems with cyclic structures, has the potential to apply to broader problems. One potential application is solving Bellman equations in Markov Decision Processes (MDPs) with sparse state transition matrixs. In an MDP, the value function v satisfies the Bellman equation $v = R + \gamma Pv$, where R is the reward vector, P is the state transition matrix, and γ is the discount factor. Rearranging this equation yields $v = (I - \gamma P)^{-1} \cdot R$, which aligns with the form in §3.3.2. A common method for evaluating the value function is through value iteration[43], which can be proved to be equivalent to the cost iteration of SimpleApp for $L(G)$. The experimental results in §5 suggest that CostApp obtains exact solutions faster than SimpleApp achieves solutions of acceptable accuracy, indicating its potential to accelerate value function computation in MDPs with sparse transitions and large state spaces. Another potential application is input-output economic modeling [26, 27, 45], where industries are interdependent with cyclic supply chains. In this model, x denotes the total production required and can be obtained by resolving a Leontief inverse: $x = (I - A)^{-1} \cdot d$, where d is a demand vector and A is an input-output matrix, which is naturally large-scale and sparse. Thus, CostApp can be directly applied to efficiently compute x on large-scale economic networks without

approximations. These examples demonstrate that CostApp can inspire the optimization of numerical solvers for large-scale sparse linear systems, making it valuable future work to explore more potential applications.

REFERENCES

- [1] [n.d.]. The audit of assertions. <https://www.accaglobal.com/us/en/student/exam-support-resources/fundamentals-exams-study-resources/f8/technical-articles/assertions.html>. Accessed: 2025-06-30.
- [2] [n.d.]. Breaking Down The Numbers: How Much Data Does The World Create Daily in 2024? <http://edgedelta.com/company/blog/how-much-data-is-created-per-day>. Accessed: 2025-09-22.
- [3] [n.d.]. Building a Simple Data Pipeline. <https://airflow.apache.org/docs/apache-airflow/stable/tutorial/pipeline.html>. Accessed: 2025-06-30.
- [4] [n.d.]. From ETL to ELT: Modernising Pipelines for High-Volume Metrics. https://www.alibabacloud.com/blog/build-and-run-an-etl-data-pipeline-and-bi-with-luigi-and-metabase-on-alibaba-cloud_598152. Accessed: 2025-06-30.
- [5] [n.d.]. Google Cloud Dataflow. <https://cloud.google.com/dataflow/docs/overview>. Accessed: 2025-06-30.
- [6] [n.d.]. Microsoft Dataflows. <https://learn.microsoft.com/en-us/power-query/dataflows/overview-dataflows-across-power-platform-dynamics-365>. Accessed: 2025-06-30.
- [7] [n.d.]. What is AWS Data Pipeline? <https://docs.aws.amazon.com/datapipeline/latest/DeveloperGuide/what-is-datapipeline.html>. Accessed: 2025-06-30.
- [8] [n.d.]. What is ETL? <https://cloud.google.com/learn/what-is-ETL?hl=en>. Accessed: 2025-06-30.
- [9] Karthik V Aadithya, Balaraman Ravindran, Tomasz P Michalak, and Nicholas R Jennings. 2010. Efficient computation of the shapley value for centrality in networks. In *International workshop on internet and network economics*. Springer, 1–13.
- [10] Réka Albert and Albert-László Barabási. 2002. Statistical mechanics of complex networks. *Reviews of modern physics* 74, 1 (2002), 47.
- [11] Alibaba Cloud. 2025. MaxCompute. https://www.alibabacloud.com/en/product/maxcompute?p_lc=1. Accessed: 2025-01-10.
- [12] Juliana Ventura Amaral and Reinaldo Guerreiro. 2019. Factors explaining a cost-based pricing essence. *Journal of Business & Industrial Marketing* 34, 8 (2019), 1850–1865.
- [13] Michael Backes, Niklas Grimm, and Aniket Kate. 2015. Data lineage in malicious environments. *IEEE Transactions on Dependable and Secure Computing* 13, 2 (2015), 178–191.
- [14] Jaeyoung Choi, Jack J Dongarra, Roldan Pozo, and David W Walker. 1992. ScaLA-PACK: A scalable linear algebra library for distributed memory concurrent computers. In *The Fourth Symposium on the Frontiers of Massively Parallel Computation*. IEEE Computer Society, 120–121.
- [15] Zicun Cong, Xuan Luo, Jian Pei, Feida Zhu, and Yong Zhang. 2022. Data pricing in machine learning pipelines. *Knowledge and Information Systems* 64, 6 (2022), 1417–1455.
- [16] Pierluigi Crescenzi, Viggo Kann, and M Halldórsson. 1995. A compendium of NP optimization problems.
- [17] Yingwei Cui and Jennifer Widom. 2003. Lineage tracing for general data warehouse transformations. *the VLDB Journal* 12, 1 (2003), 41–58.
- [18] Guy Even. 1995. Joseph (Seffi) Naor, Baruch Schieber, and Madhu Sudan. *Approximating minimum feedback sets and multi-cuts in directed graphs*. Integer Programming and Combinatorial Optimization (1995), 14–28.
- [19] Drew Fudenberg and J Miguel Villas-Boas. 2012. Price discrimination in the digital economy. (2012).
- [20] Robert Ikeda and Jennifer Widom. 2009. Data lineage: A survey. *Stanford University Publications*. <http://ilpubs.stanford.edu:8090/918> (2009), 1.
- [21] Gabriela Jacques-Silva, Evangelia Kalyvianaki, Katriel Cohn-Gordon, Adham Meguid, Huy Nguyen, Danny Ben-David, Carl Nayak, Varun Saravagi, George Stasa, Ioannis Papagiannis, et al. 2025. Unified Lineage System: Tracking Data Provenance at Scale. In *Companion of the 2025 International Conference on Management of Data*. 457–470.
- [22] Ruoxi Jia, David Dao, Boxin Wang, Frances Ann Hubis, Nick Hynes, Nezihe Merve Gürel, Bo Li, Ce Zhang, Dawn Song, and Costas J Spanos. 2019. Towards efficient data valuation based on the shapley value. In *The 22nd International Conference on Artificial Intelligence and Statistics*. PMLR, 1167–1176.
- [23] Charles I Jones and Christopher Tonetti. 2020. Nonrivalry and the Economics of Data. *American Economic Review* 110, 9 (2020), 2819–2858.
- [24] Nicola Jones. 2024. The AI revolution is running out of data. What can researchers do? *Nature* 636, 8042 (2024), 290–292.
- [25] Richard M Karp. 1972. Reducibility among combinatorial problems. In *Complexity of computer computations*. Springer, 85–103.
- [26] Wassily Leontief. 1974. Structure of the world economy: Outline of a simple input-output formulation. *The American Economic Review* 64, 6 (1974), 823–834.
- [27] Wassily Leontief. 1986. *Input-output economics*. Oxford University Press.
- [28] Jinfei Liu, Jian Lou, Junxu Liu, Li Xiong, Jian Pei, and Jimeng Sun. 2021. Dealer: an end-to-end model marketplace with differential privacy. *Proceedings of the VLDB Endowment* 14, 6 (2021).
- [29] Rui Liu, Kwanghyun Park, Fotis Psallidas, Xiaoyong Zhu, Jinghui Mo, Rathijit Sen, Matteo Interlandi, Konstantinos Karanatos, Yuan Yuan Tian, and Jesús Camacho-Rodríguez. 2023. Optimizing Data Pipelines for Machine Learning in Feature Stores. *Proceedings of the VLDB Endowment* 16, 13 (2023), 4230–4239.
- [30] Chenghao Lyu, Qi Fan, Fei Song, Arnab Sinha, Yanlei Diao, Wei Chen, Li Ma, Yihui Feng, Yaliang Li, Kai Zeng, et al. 2022. Fine-Grained Modeling and Optimization for Intelligent Resource Management in Big Data Processing. In *VLDB 2022-48th International Conference on Very Large Databases*, Vol. 15.
- [31] Jeffrey K MacKie-Mason, Juan F Riveros, and Robert S Gazzale. 2000. Pricing and bundling electronic information goods: Experimental evidence. MIT Press.
- [32] Grzegorz Malewicz, Matthew H Austern, Aart JC Bik, James C Dehnert, Ilan Horn, Naty Leiser, and Grzegorz Czajkowski. 2010. Pregel: a system for large-scale graph processing. In *Proceedings of the 2010 ACM SIGMOD International Conference on Management of data (SIGMOD)*. 135–146.
- [33] Aliomar Lino Mattos, JosÃ Oyadomari, Fernando Nascimento Zatta, et al. 2021. Pricing Research: State of the Art and Future Opportunities. *SAGE Open* 11, 3 (2021).
- [34] Xiangrui Meng, Joseph Bradley, Burak Yavuz, Evan Sparks, Shivaram Venkataraman, Davies Liu, Jeremy Freeman, DB Tsai, Manish Amde, Sean Owen, et al. 2016. Mllib: Machine learning in apache spark. *Journal of Machine Learning Research* 17, 34 (2016), 1–7.
- [35] Aiswarya Raj Munappy, Jan Bosch, and Helena Homström Olsson. 2020. Data pipeline management in practice: Challenges and opportunities. In *Product-Focused Software Process Improvement: 21st International Conference, PROFES 2020, Turin, Italy, November 25–27, 2020, Proceedings 21*. Springer, 168–184.
- [36] Andrew Odlyzko. 2003. Privacy, economics, and price discrimination on the internet. In *Proceedings of the 5th international conference on Electronic commerce*. 355–366.
- [37] Jian Pei. 2020. A survey on data pricing: from economics to data science. *IEEE Transactions on Knowledge and Data Engineering (TKDE)* 34, 10 (2020), 4586–4608.
- [38] Jian Pei, Raul Castro Fernandez, and Xiaohui Yu. 2023. Data and ai model markets: Opportunities for data and model sharing, discovery, and integration. *Proceedings of the VLDB Endowment* 16, 12 (2023), 3872–3873.
- [39] Carl Shapiro. 1999. *Information rules: A strategic guide to the network economy*. Harvard Business School Press.
- [40] Carl Shapiro and Hal R Varian. 1998. Versioning: the smart way to sell information. *Harvard business review* 107, 6 (1998), 107.
- [41] Tapan Srivastava and Raul Castro Fernandez. 2024. Saving Money for Analytical Workloads in the Cloud. *Proceedings of the VLDB Endowment* 17, 11 (2024), 3524–3537.
- [42] Yutian Sun, Tim Meehan, Rebecca Schlussel, Wenlei Xie, Masha Basanova, Orri Erling, Andrii Rosa, Shixuan Fan, Rongrong Zhong, Arun Thirupathi, et al. 2023. Presto: A decade of SQL analytics at Meta. *Proceedings of the ACM on Management of Data* 1, 2 (2023), 1–25.
- [43] R.S. Sutton and A.G. Barto. 2018. *Reinforcement Learning, second edition: An Introduction*. MIT Press. <https://books.google.com.br/books?id=sWV0DwAAQBAJ>
- [44] Jan Vincent Szlang, Sebastian Bress, Sebastian Cattes, Jonathan Dees, Florian Funke, Max Heimel, Michel Oleynik, Ismail Oukid, and Tobias Maltenberger. 2025. Workload Insights from the Snowflake Data Cloud: What Do Production Analytic Queries Really Look Like? *Proceedings of the VLDB Endowment* 18, 12 (2025), 5126–5138.
- [45] Thijs Ten Raa. 2009. *Input-output economics: Theory and applications-featuring Asian economies*. World Scientific.
- [46] Caesar Wu, Rajkumar Buyya, and Kotagiri Ramamohanarao. 2019. Cloud pricing models: Taxonomy, survey, and interdisciplinary challenges. *ACM Computing Surveys (CSUR)* 52, 6 (2019), 1–36.
- [47] Jiayao Zhang, Yuran Bi, Mengye Cheng, Jinfei Liu, Kui Ren, Qiheng Sun, Yihang Wu, Yang Cao, Raul Castro Fernandez, Haifeng Xu, et al. 2024. A Survey on Data Markets. *arXiv preprint arXiv:2411.07267* (2024).
- [48] Mark Zhao, Emanuel Adamak, and Christos Kozyrakis. 2024. cedar: Optimized and Unified Machine Learning Input Data Pipelines. *Proceedings of the VLDB Endowment* 18, 2 (2024), 488–502.
- [49] Mark Zhao, Niket Agarwal, Aarti Basant, Buğra Gedik, Satadru Pan, Mustafa Ozdal, Rakesh Komuravelli, Jerry Pan, Tianshu Bao, Haowei Lu, et al. 2022. Understanding data storage and ingestion for large-scale deep recommendation model training: Industrial product. In *Proceedings of the 49th annual international symposium on computer architecture*. 1042–1057.